Hydrology Research

British Hydrological Society

IWA PUBLISHING

Hydrology Research Vol 55 No 10, 1030 doi: 10.2166/nh.2024.054

Determination of the coefficient of friction in the penstock of a hydro-electric dam: Application of two approaches

Moukam Tchawe Tchawe [a,*], François Nkontchou Ngongang[a], Max-well Tientcheu Nsiewe[b], Thomas Djiako[c], Dénis Tcheukam-Toko[d] and Bienvenu Kenmeugne[e]

[a] Department of Mechanical Engineering, ENSAI, University of Ngaoundere, Ngaoundere, Cameroon
[b] Department of Fundamental Sciences, EGCIM, University of Ngaoundere, Ngaoundere, Cameroon
[c] Department of Mechanical Engineering and Energy, ISTA, University Institute of the Gulf of Guinea, Douala, Cameroon
[d] Department of Mechanical Engineering, COT, University of Buea, Buea, Cameroon
[e] Department of Mechanical Engineering, ENSPY, University of Yaounde 1, Yaounde, Cameroon
*Corresponding author. E-mail: moukam.tchawe@univ-ndere.cm

MT, 0000-0001-5449-7954

ABSTRACT

Several formulae of the coefficient of friction have emerged after that of Nikuradse such as the Colebrook–White formula adopted for the calculation of the coefficient of friction in penstocks. However, this requires enormous computing resources because it suffers from an implicit nature. Other authors have proposed explicit formulae for this in order to reduce calculation times and make applications easy. Among these authors, the most used are the formulae of Swamee–Jain and Haaland. In this work, we set out to study the evolution of friction on the top, bottom and side walls of a penstock using these two formulas. The objective is to find which one best characterizes the friction and gives results close to the implicit Colebrook–White formula. To carry out this work, the study was made by a numerical approach in FLUENT. It appears that the Swamee–Jain correlation gives values closer to that of Colebrook–White along the walls. On the side walls, Haaland's formula better describes the constancy of friction with a much larger range of values than Swamee–Jain. On the upper and lower walls, the friction has a linear character.

Key words: boundary layer, CFD, friction coefficient, hydroelectric dam, penstock

HIGHLIGHTS

- The Colebrook–White equation is adopted for calculating the coefficient of friction in pipelines.
- The Colebrook–White equation serves as a reference formula for the calculation of the coefficient of friction in the conduits.
- We propose to determine from the Haaland and Swamee-Jain formulae.
- The Three Gorges Dam in China was studied.

INTRODUCTION

A dam is an engineering structure built across a watercourse and intended to regulate its flow and/or to store water to allow a desired flow. The water retained by the dam is channeled to the turbine using the penstock, which is the site of several physical phenomena. The flow is still turbulent there (Elie 2014) and the pressure drops in the case of small dams are around 15%, of which the most important are due to friction (Chapallaz *et al.* 1995). As a result, friction becomes a key parameter to be controlled in order to guarantee and maintain the structure's performance.

The coefficient of friction is associated with this key parameter and depends both on the Reynolds number that identifies the flow regime and on the roughness of the internal wall of the penstock. The 1937 Colebrook–White equation is adopted for calculating the coefficient of friction in pipelines, given its applicability over a wide range of flow regimes and roughness values. Note that this equation follows from the development of Prandtl for smooth pipes (Prandtl 1932) and from that of Von Karman for rough pipes (Von Karman 1934). Since its publication, it has become the reference formula for calculating the coefficient of friction in large-diameter pipes. However, its use is tedious because it is an implicit equation.

In order to overcome the implicit form of this equation, a certain number of explicit functions have been developed to approach it. These equations are all constant functions and do not take into account any other parameter apart from Reynolds number, length and relative roughness. In fact, this aspect is the subject of a work we are developing and which will be published in the near future.

In this article, we propose to determine from the Haaland formulae, then from Swamee–Jain's, the coefficient of friction in the penstock of a dam by a numerical approach (via the CFD method). The aim is to determine which of these two explicit expressions best approximates the Colebroock–White formula and also to observe which appears to be sensitive to any variation in the penstock. To this end, the dam used for the application of our approach is the Three Gorges Dam in China, with a diameter of 12.4 m and made up of three sections. Note that the flow is not symmetrical in all directions in this penstock (Wang *et al.* 2012).

MATERIALS AND METHODS

Figure 1 shows the model of our structure with a penstock 12.4 m in diameter and 65 m in length.

The work is done on the three sections constituting the penstock with its maximum flow rate of 970 m^3/s:

- The first section is located between the water intake and the first bend;
- The second section is located between the two elbows;
- The third section is located between the second bend and the turbine inlet.

Our work is based on the CFD method, with modeling of our structure in Gambit 2.4 software and simulation in Fluent 6.3.26 software. The turbulence model used is $k-\varepsilon$ realizable because it is well suited to boundary layers with a strong adverse pressure gradient, to strong curvature and vortex flows, and finally is considered isotropic. The second order equations are solved with the velocity-pressure coupling method SIMPLEC and a convergence criterion 10^{-6}. The approach flow is stationary, the function near walls function considered in the software is the standard wall function, and the discretization scheme is Body Force Weighted.

General equation of the problem

The equations that govern turbulent hydrodynamic flows are the laws of conservation of mass, momentum and energy. The flow in our case is considered to be isothermal. The fluid is assumed to be a Newtonian fluid. The flow is incompressible and isothermal with constant viscosity, and can be described by the velocity and pressure field governed by the Navier–Stokes

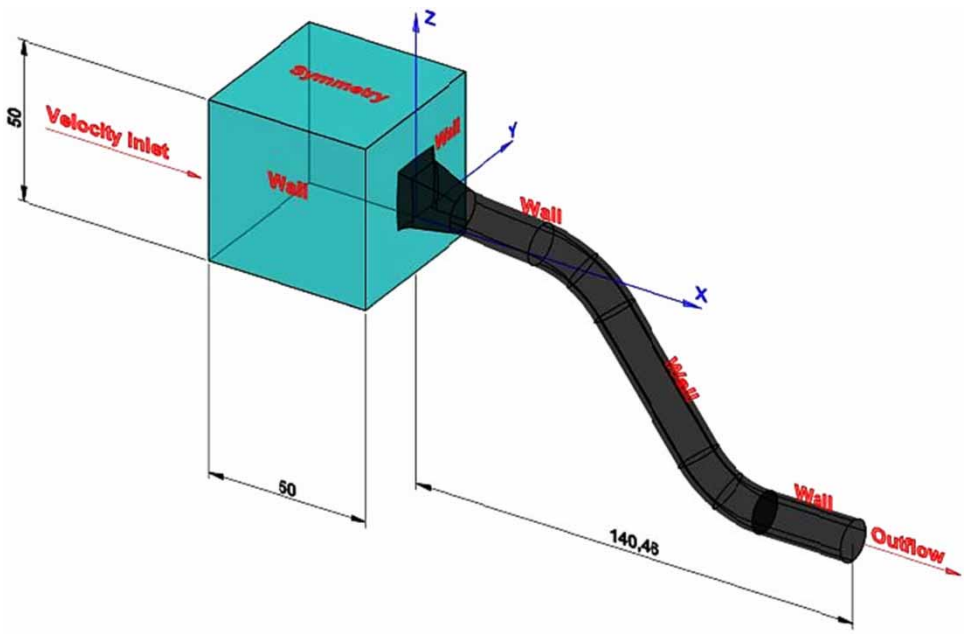

Figure 1 | Study area (Penstock with approach tank).

equations (Von Karman 1934; Wilcox 1998) cited by Ketcheuzeu-Ngakam *et al.* (2014) and Tchawe *et al.* (2015, 2018):

$$\frac{\partial U_i}{\partial U_j} = 0 \tag{1}$$

The dynamic conservation is:

$$\frac{\partial U_i}{\partial t} + \frac{\partial (U_j U_i)}{\partial x_j} = \frac{1}{\rho}\left(-\frac{\partial p}{\partial x_i} + \frac{\partial \tau_{ij}}{\partial x_i}\right) \tag{2}$$

where U_i represents the velocities in x_i coordinate directions; p is the static pressure load, ρ the constant density, and τ_{ij} the viscous stress tensor. For a Newtonian fluid:

$$\tau_{ij} = \mu\left(\frac{\partial U_i}{\partial x_j} + \frac{\partial U_j}{\partial x_i}\right) \tag{3}$$

In the flows, the variations are too rapid to be described in time and space. Velocity details are lost. We can adopt the following decomposition for the pressure and the velocity:

$$u_i = \overline{u_i} + u_i' \tag{4}$$

where $\overline{u_i}$ and u_i' are the average components of the fluctuating velocity ($i = 1, 2, 3$). In the same way for the pressure and the other scalar values:

$$\phi = \bar{\phi} + \phi' \tag{5}$$

where ϕ represents a scalar such as pressure, energy, or other concentration.

Substituting expressions of this form for the flow variables in the instantaneous continuity and momentum equations while taking a time average, we obtain the average momentum equations. They can be written in the form of Cartesian tensor:

$$\frac{\partial \rho}{\partial t} + \frac{\partial}{\partial x_i}(\rho u_i) = 0 \tag{6}$$

$$\frac{\partial}{\partial t}(\rho u_i) + \frac{\partial}{\partial x_i}(\rho u_i u_j) = -\frac{\partial p}{\partial x_i} + \frac{\partial}{\partial x_j}\left[\mu\left(\frac{\partial u_i}{\partial x_j} + \frac{\partial u_j}{\partial x_i} + \frac{2}{3}\delta_{ij}\frac{\partial u_l}{\partial x_l}\right)\right] + \frac{\partial}{\partial x_j}(-\rho\overline{u'_i u'_j}) \tag{7}$$

Additional terms now appear that represent the effects of turbulence. The Reynolds stress $\rho\overline{u'_i u'_j}$, must be modeled to close the equation. The closing of the equation uses Boussinesq's approximation (Boussinesq 1877):

$$-\rho\overline{u'_i u'_j} = \mu\left(\frac{\partial u_i}{\partial x_j} + \frac{\partial u_j}{\partial x_i}\right) - \frac{2}{3}\left(\rho k + \mu_t \frac{\partial u_i}{\partial x_i}\right)\delta_{ij} \tag{8}$$

The model of the transport equations for k and ε is:

$$\frac{\partial}{\partial t}(\rho k) + \frac{\partial}{\partial x_i}(\rho k U_j) = \frac{\partial}{\partial x_i}\left[\left(\mu + \frac{\mu_t}{\sigma_k}\right)\frac{\partial k}{\partial x_j}\right] + G_k + G_b + \rho\varepsilon + Y_M + S_k \tag{9a}$$

$$\frac{\partial}{\partial t}(\rho\varepsilon) + \frac{\partial}{\partial x_j}(\rho\varepsilon U_j) = \frac{\partial}{\partial x_j}\left[\left(\mu + \frac{\mu_t}{\sigma_\varepsilon}\right)\frac{\partial \varepsilon}{\partial x_j}\right] + \rho C_1 S_\varepsilon + \rho C_2 \frac{\varepsilon^2}{k + \sqrt{\nu\varepsilon}} + C_{1\varepsilon}\frac{\varepsilon}{k} C_{3\varepsilon} G_b + S_\varepsilon \tag{9b}$$

where $C_1 = \max[0, 43(\eta/\eta + 5)]$; $\eta = S_\varepsilon^k$; $C_{3\varepsilon} = \tanh\left[\frac{\nu}{u}\right]$

$\boldsymbol{C_{3\varepsilon}}$ represents the degree of influence of volume forces, $\boldsymbol{\nu}$ is the component of the flow velocity parallel to the gravitational vector, and u is the component of the flow velocity perpendicular to the gravitational vector.

In these equations, $G_k = -\rho\overline{u'_i u'_j}(\partial u_j/\partial x_i)$ represents the generator term of the kinetic energy of turbulence due to the mean of the calculated velocity gradient, $G_b = \beta g_i(\mu_t/P_{rt})(\partial T/\partial x_i)$ is the generator term of the kinetic energy of turbulence due to the volume forces, Y_M represents the fluctuation of the expansion in compressible turbulence. C_1 and C_2 are their constants. σ_k et σ_ε are the turbulent Prandtl numbers for k and ε respectively. S_k and S_ε are user-defined terms.

The turbulent viscosity is given by:

$$\mu_t = \rho C_\mu \frac{k^2}{\varepsilon} \tag{10}$$

The difference between the three models is in the term of C_μ which is given by:

$$C_\mu = \frac{1}{A_0 + A_S(kU^*/\varepsilon)} \tag{11}$$

The constants are given by:

$$A_0 = 4,04\ ;\ A_S = \sqrt{6}cos\phi$$

$$C_{1\varepsilon} = 1,44;\ C_2 = 1,9\ ;\ \sigma_k 1,0\ ;\ \sigma_\varepsilon = 1,2$$

Friction coefficient equation

Swamee & Jain (1976) developed the explicit relation to determining the coefficient of friction as a function of Reynolds number (Re) and relative roughness (ε/D), from the Colebrook–White relation according to the following equation:

$$f = 0,25\log\left(\frac{\varepsilon}{3,7D} + \frac{5,74}{0,9R_e}\right)^{-2} \tag{12}$$

Haaland (1983) also proposes a correlation for the calculation of friction by:

$$\frac{1}{\sqrt{f}} = -1,8\log\left(\frac{6,9}{R_e} + \left(\frac{\varepsilon}{3,7D}\right)^{1,11}\right) \tag{13}$$

RESULTS

Our study is essentially based on the phenomena occurring near the walls. We made a third degree smoothing close to the walls to reduce calculation errors and the cells are regular tetrahedral (Figure 2).

The results thus obtained will be presented on the lower (bottom), upper (top) and side walls as a function of the Reynolds number, for each of the three sections that constitute our penstock.

First section

We first note that the maximum coefficient of friction is not observed at the same height in the penstock on each wall considered in the section.

Bottom wall

The average height for the maximum coefficient of friction on this wall is observed at ≈ 20 mm from the wall as shown in Figures 3(a) and 3(b):

We note from these curves that the evolution of the coefficient of friction at this scale is substantially linear for the Swamee–Jain formula and that of Haaland. However, Haaland's formula is more sensitive to the effects on the walls.

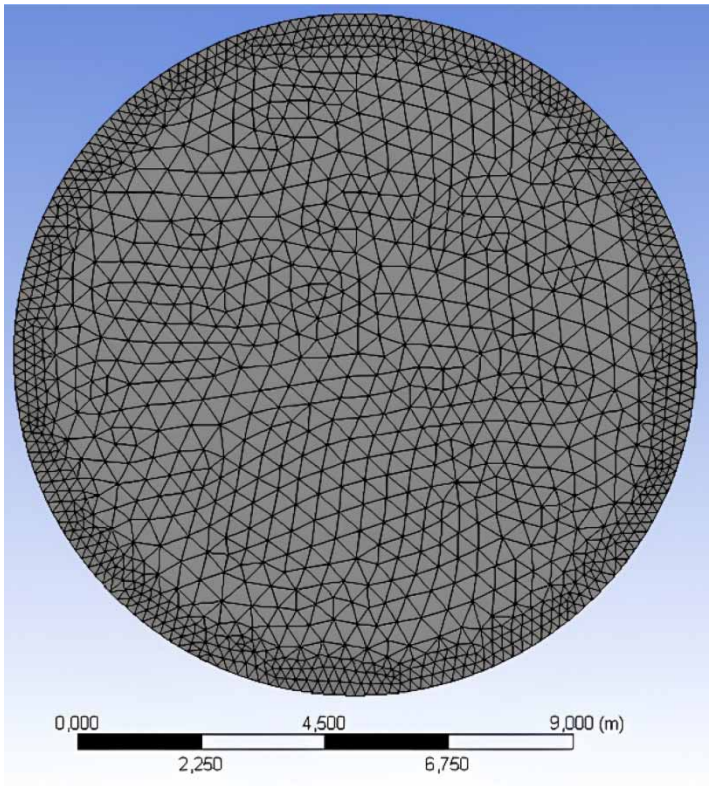

Figure 2 | Mesh structure: cross-section (present study).

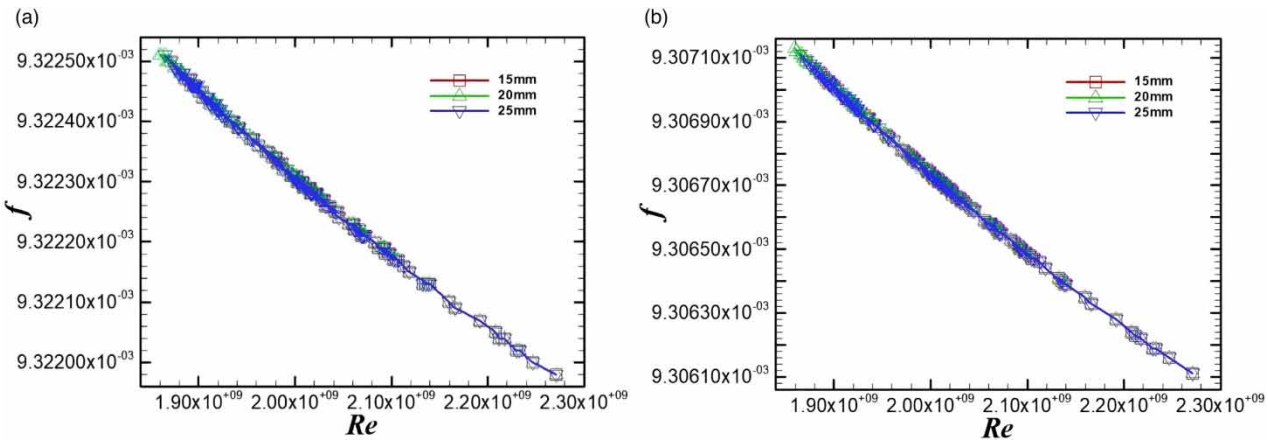

Figure 3 | Evolution of the friction coefficient on the lower wall of the first section according to: (a) Haaland's formula and (b) Swamee–Jain formula.

Upper wall

Here, the average height for the maximum coefficient of friction is observed at ≈ 2 mm from the wall as shown in Figures 4(a) and 4(b).

We also observe that the observation made for the lower wall is practically the same for the upper wall.

Side wall

For the side wall, the average height for the maximum coefficient of friction is observed at ≈ 4 mm from the wall as shown in Figures 5(a) and 5(b).

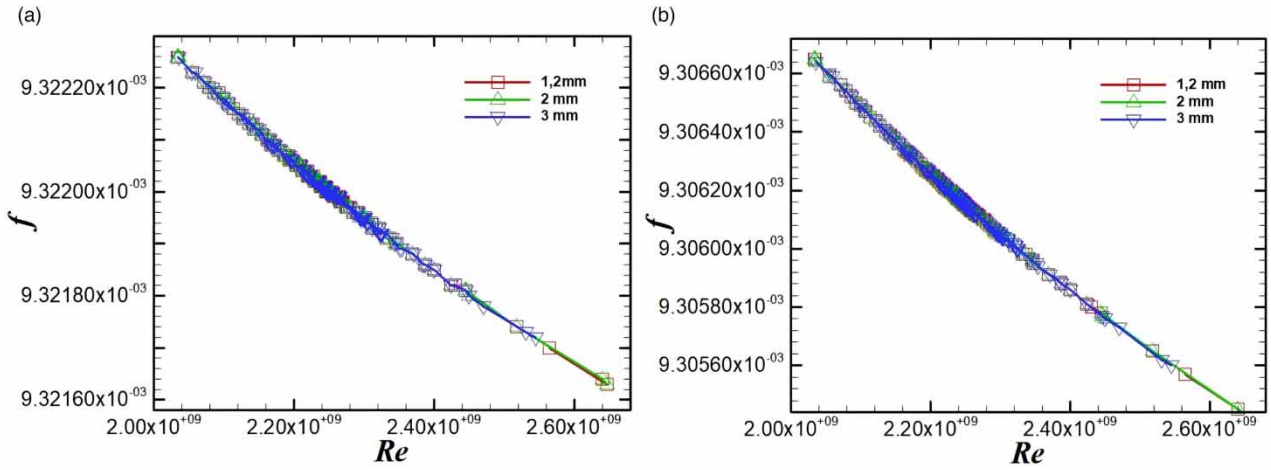

Figure 4 | Evolution of the coefficient of friction on the top wall of the first section according to: (a) the Haaland's formula and (b) Swamee–Jain formula.

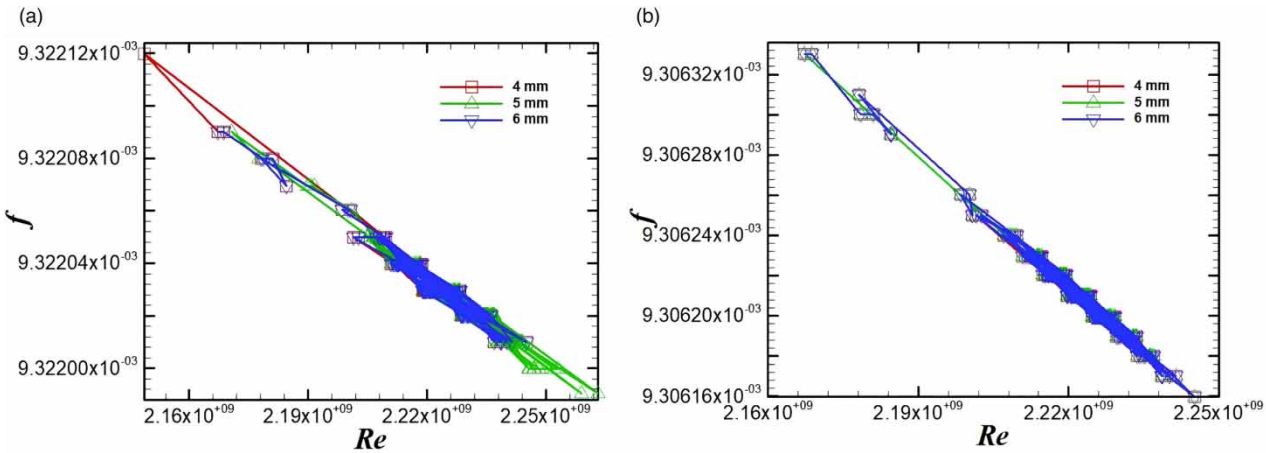

Figure 5 | Evolution of the friction coefficient on the side wall of the first section according to: (a) Haaland's formula and (b) Swamee–Jain formula.

The sensitivity noted above in Haaland's formula is more noticeable at this level. The exact value of the coefficient of friction is difficult to observe for a given velocity. Although the Swamee–Jain formula presents a more attenuated form of the coefficient of friction at the same given velocity, it is no less unpredictable.

It thus emerges that the maximum height for a maximum value of coefficient of friction for this section is approximately $\leq$20 mm.

Second section

This section has the particularity of being the most inclined of the sections. Thus, the structure of the inlet flow is conditioned by the geographical arrangement of the first section and the shape of the elbow.

Bottom wall

The average height for the maximum coefficient of friction on this wall is observed at $\approx$ 60 mm from the wall as shown in Figures 6(a) and 6(b).

We note from these curves that the evolution of the coefficient of friction is still substantially linear for the two formulas. The results are even more or less identical for the two formulas on this scale.

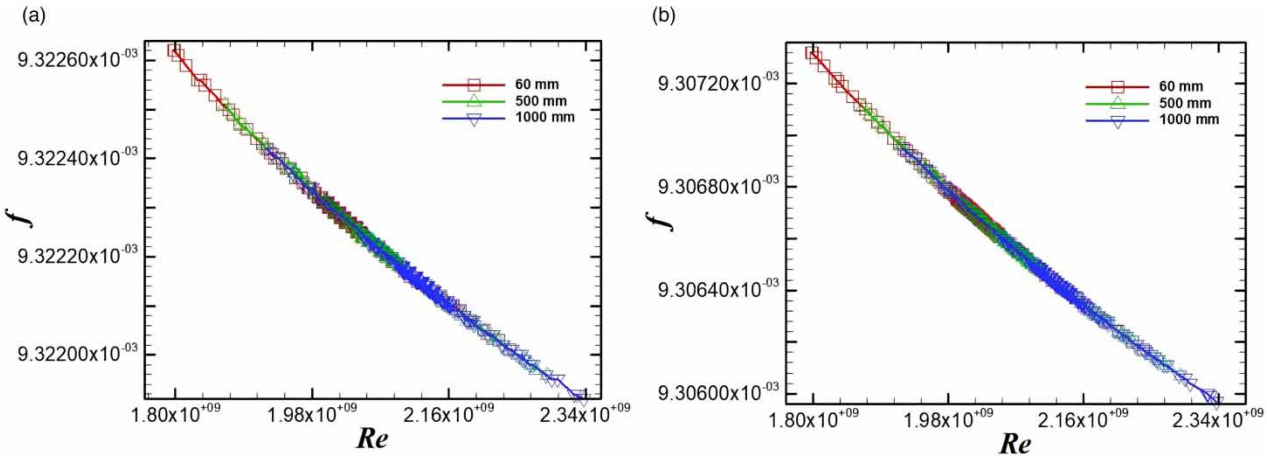

Figure 6 | Evolution of the coefficient of friction on the bottom wall of the second section according to: (a) Haaland's formula and (b) Swamee–Jain formula.

Upper wall

Unlike the first portion, the average height for the maximum coefficient of friction is observed at ≈ 1.2 mm from the wall as shown in Figures 7(a) and 7(b).

From these figures, the finding is the same as that noted on the lower wall of this portion, with a slight fluctuation observed for the maximum velocity in Haaland's formula.

Side wall

The average height for the maximum coefficient of friction is observed at ≈ 5 mm from the wall for this section, as shown in Figures 8(a) and 8(b).

The same observation is made when determining the friction coefficient on the side wall of the first section. Haaland's formula still presents its more sensitive character than Swamee–Jain's. The maximum height for a value of the maximum friction coefficient is substantially ≤60 mm in this section.

Third section

Unlike the other two sections, this one is laid out horizontally and has the particularity of being just upstream of the turbine. The efficiency of the turbine depends on the characteristics resulting directly from it.

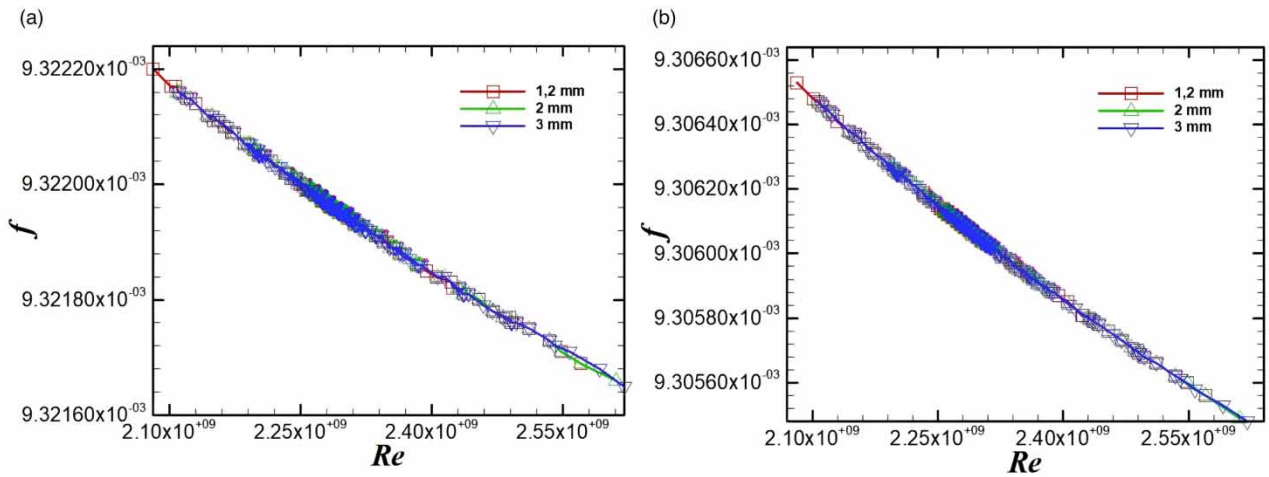

Figure 7 | Evolution of the friction coefficient on the upper wall of the second section according to: (a) Haaland's formula and (b) Swamee–Jain formula.

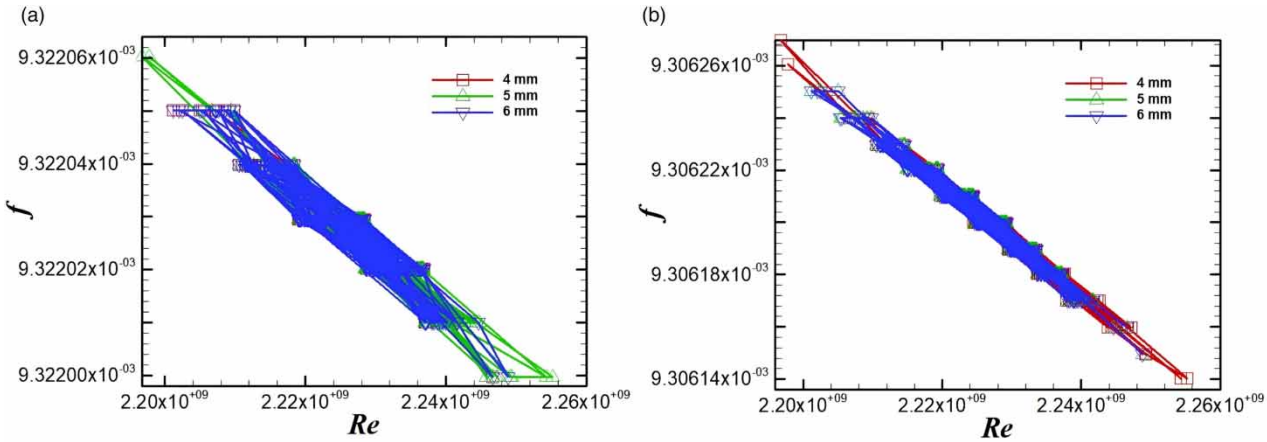

Figure 8 | Evolution of the friction coefficient on the side wall of the second section according to: (a) Haaland's formula and (b) Swamee–Jain formula.

Bottom wall

The average height for the maximum coefficient of friction on this wall is observed at ≈ 1.2 mm from the wall as shown in Figures 9(a) and 9(b).

The two formulas describe substantially the same behavior on this wall as noted in the case of the preceding sections.

Upper wall

The average height for the maximum coefficient of friction on this wall was observed at ≈ 3 mm from the wall as shown in Figures 10(a) and 10(b).

Likewise, a sensitivity was observed in the result obtained from Haaland's formula compared to Swamee–Jain.

Side wall

The average height for the maximum coefficient of friction is always observed at ≈ 5 mm from the wall for this section, as shown in Figures 11(a) and 11(b).

As for the first two sections, the observation is the same when we highlight the coefficient of friction on the side wall. Haaland's formula always presents a more sensitive character than that of Swamee–Jain. The average height for a value of the maximum coefficient of friction is this time substantially ≤5 mm in this section.

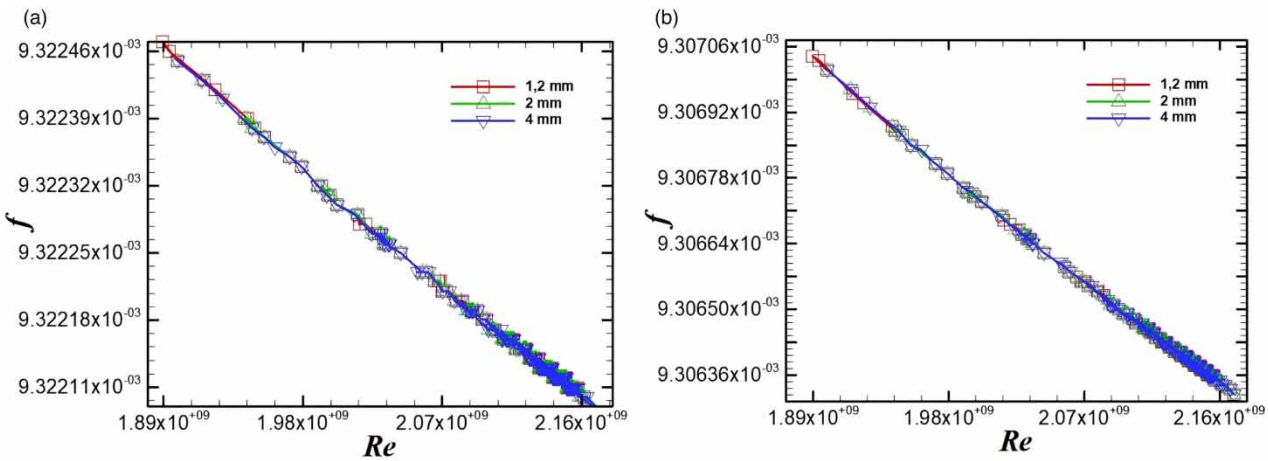

Figure 9 | Evolution of the friction coefficient on the bottom wall of the third section according to: (a) Haaland's formula and (b) Swamee–Jain formula.

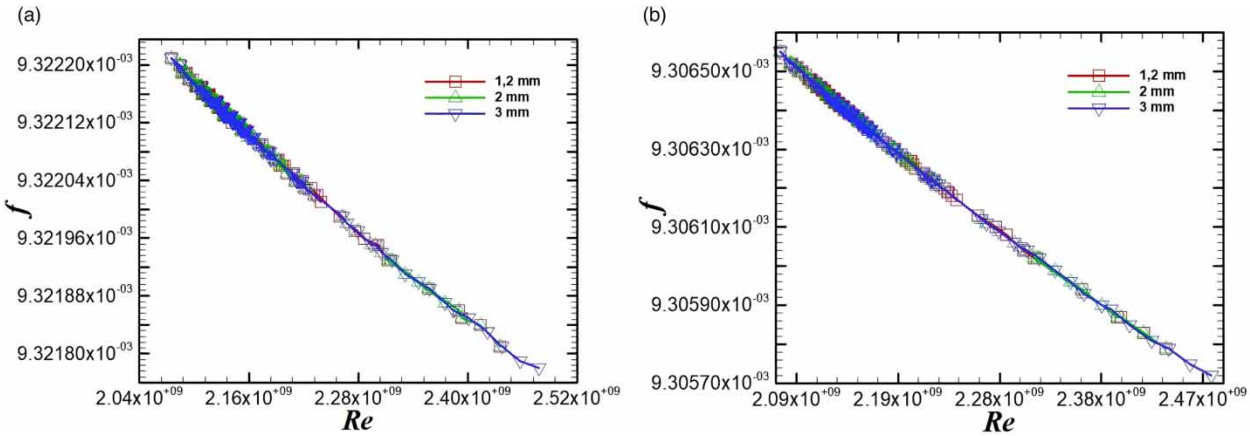

Figure 10 | Evolution of the friction coefficient on the top wall of the third section according to: (a) Haaland's formula and (b) Swamee–Jain formula.

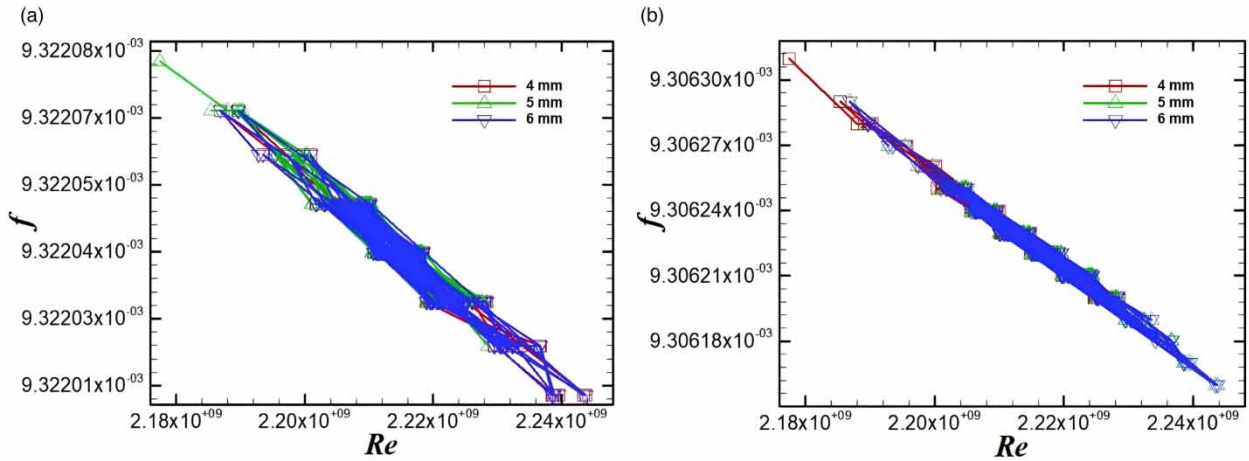

Figure 11 | Evolution of the friction coefficient on the side wall of the third section according to: (a) Haaland's formula and (b) Swamee–Jain formula.

To better appreciate the different results, a numerical calculation was carried out with the formula proposed by Colebrook–White (1937, 1939). The different results are shown in Tables 1–3, with the thicknesses of the boundary layers found for each correlation.

We notice in these tables on one hand the differences between the results of the coefficient of friction obtained by the Colebrook–White formula and those of the two other formulae. It is of the order of 10^{-6} for the Swamee–Jain formula and of the order of 10^{-5} for the Haaland formula. Regarding the thicknesses at which the friction is maximum, the Swamee–Jain correlation gives substantially identical results for different velocities on the bottom and upper walls. On the other hand, these thicknesses vary as a function of the velocity in the Haaland correlation. Regarding the side wall, the two formulas give the same height for the friction coefficient.

DISCUSSION

Winning & Coole (2015) propose an improved method to determine the coefficient of friction in pipes by mathematical calculations. They calculate the mean square error (MSE), the mean relative error in percentage (ERMP) and the mean time required to perform 300 million calculations using random input values obtained in 28 explicit equations examined. These equations and the results of the calculations are listed in Table 4.

Table 1 | Thickness corresponding to the maximum friction coefficient in the first section

		Formulas					Difference	
		Haaland		Swamee–Jain				
Walls	Velocity (m/s)	Thickness (mm)	f_{max}	Thickness (mm)	f_{max}	Colebrook–White	Haaland	Swamee–Jain
Bottom	7	20	9.32337×10^{-3}	20	9.30871×10^{-3}	9.30201×10^{-3}	2.136×10^{-5}	6.696×10^{-6}
	8	20–25	9.32262×10^{-3}	20	9.30779×10^{-3}	9.30201×10^{-3}	2.061×10^{-5}	5.785×10^{-6}
	9	20–25	9.32251×10^{-3}	20	9.30713×10^{-3}	9.30200×10^{-3}	2.051×10^{-5}	5.132×10^{-6}
Upper	7	0.05–2	9.32304×10^{-3}	0.05–2	9.30810×10^{-3}	9.30201×10^{-3}	2.103×10^{-5}	6.086×10^{-6}
	8	0.05–3	9.32259×10^{-3}	0.05–3	9.30727×10^{-3}	9.30201×10^{-3}	2.058×10^{-5}	5.265×10^{-6}
	9	0.05–4	9.32226×10^{-3}	0.05–1.2	9.30665×10^{-3}	9.30200×10^{-3}	2.026×10^{-5}	4.652×10^{-6}
Side	7	0.05–4	9.32285×10^{-3}	0.05–4	9.30775×10^{-3}	9.30201×10^{-3}	2.084×10^{-5}	5.736×10^{-6}
	8	0.05–4	9.32243×10^{-3}	0.05–4	9.30696×10^{-3}	9.30201×10^{-3}	2.042×10^{-5}	4.955×10^{-6}
	9	0.05–4	9.32212×10^{-3}	0.05–4	9.30637×10^{-3}	9.30200×10^{-3}	2.012×10^{-5}	4.372×10^{-6}

Table 2 | Thickness corresponding to the maximum friction coefficient in the second section

		Formulas					Difference	
		Haaland		Swamee–Jain				
Walls	Velocity (m/s)	Thickness (mm)	f_{max}	Thickness (mm)	f_{max}	Colebrook–White	Haaland	Swamee–Jain
Bottom	7	0.05–70	9.32349×10^{-3}	0.05–70	9.30894×10^{-3}	9.30201×10^{-3}	2.148×10^{-5}	6.926×10^{-6}
	8	0.05–70	9.32265×10^{-3}	0.05–70	9.30801×10^{-3}	9.30201×10^{-3}	2.064×10^{-5}	6.005×10^{-6}
	9	0.05–70	9.32262×10^{-3}	0.05–70	9.30732×10^{-3}	9.30200×10^{-3}	2.062×10^{-5}	5.322×10^{-6}
Upper	7	0.05–1.2	9.32296×10^{-3}	0.05–1,2	9.30795×10^{-3}	9.30201×10^{-3}	2.095×10^{-5}	5.936×10^{-6}
	8	0.05–1.2	9.32195×10^{-3}	0.05–1,2	9.30713×10^{-3}	9.30201×10^{-3}	1.994×10^{-5}	5.125×10^{-6}
	9	0.05–1.2	9.32220×10^{-3}	0.05–1,2	9.30653×10^{-3}	9.30200×10^{-3}	2.020×10^{-5}	4.532×10^{-6}
Side	7	0.05–4	9.32277×10^{-3}	0.05–4	9.30761×10^{-3}	9.30201×10^{-3}	2.076×10^{-5}	5.596×10^{-6}
	8	0.05–70	9.32236×10^{-3}	0.05–70	9.30683×10^{-3}	9.30201×10^{-3}	2.035×10^{-5}	4.825×10^{-6}
	9	5	9.32206×10^{-3}	5	9.30627×10^{-3}	9.30199×10^{-3}	2.006×10^{-5}	4.272×10^{-6}

Table 3 | Thickness corresponding to the maximum friction coefficient in the third section

		Formulas					Difference	
		Haaland		Swamee–Jain				
Walls	Velocity (m/s)	Thickness (mm)	f_{max}	Thickness (mm)	f_{max}	Colebrook–White	Haaland	Swamee–Jain
Bottom	7	0.05–2	9.32329×10^{-3}	0.05–1.2	9.30859×10^{-3}	9.30201×10^{-3}	2.128×10^{-5}	6.576×10^{-6}
	8	0.05–60	9.32282×10^{-3}	0.05	9.30770×10^{-3}	9.30201×10^{-3}	2.081×10^{-5}	5.695×10^{-6}
	9	0.05–2	9.32247×10^{-3}	0.05–2	9.30701×10^{-3}	9.30200×10^{-3}	2.047×10^{-5}	5.012×10^{-6}
Upper	7	0.05–2	9.32296×10^{-3}	0.05–3	9.30797×10^{-3}	9.30201×10^{-3}	2.095×10^{-5}	5.956×10^{-6}
	8	0.05–3	9.32253×10^{-3}	0.05–3	9.30715×10^{-3}	9.30201×10^{-3}	2.052×10^{-5}	5.145×10^{-6}
	9	0.05–1.2	9.32221×10^{-3}	0.05–3	9.30655×10^{-3}	9.30200×10^{-3}	2.021×10^{-5}	4.552×10^{-6}
Side	7	0.05–70	9.32279×10^{-3}	0.05–70	9.30765×10^{-3}	9.30201×10^{-3}	2.078×10^{-5}	5.636×10^{-6}
	8	0.05–70	9.32238×10^{-3}	0.05–70	9.30686×10^{-3}	9.30201×10^{-3}	2.037×10^{-5}	4.855×10^{-6}
	9	5	9.32208×10^{-3}	5	9.30631×10^{-3}	9.30200×10^{-3}	2.008×10^{-5}	4.312×10^{-6}

From this table, it can be seen that the Swamee–Jain equation, although more widely used in industry according to Achour & Bedjaoui (2006), is neither more efficient nor faster. The same is true for the Haaland equation. However, they are the ones that offer the mean of the weakest squares. These results show us that Haaland's formula is precise with a low ERMP, but less

Table 4 | Explicit equations examined and results found

Equation	MSE	ERMP	Mean time
Sonnad & Goudar (2006)	1.05×10^{-8}	0.174	0.5999
Schorle *et al.* (1980)	3.83×10^{-9}	0.125	0.6224
Zigrang & Sylvester (1982), Eq. (11)	3.10×10^{-9}	0.141	0.6343
Seghides (1984), Eq. (3)	1.89×10^{-10}	0.037	0.6463
Jain (1976)	1.33×10^{-7}	0.452	0.6016
Haaland (1983)	2.67×10^{-8}	0.373	0.6326
Fang *et al.* (2011)	6.55×10^{-9}	0.156	0.6411
Swamee & Jain (1976)	1.61×10^{-7}	0.478	0.5931
Seghides (1984), Eq. (2)	7.51×10^{-12}	0.006	0.6582
Churchill (1973)	1.68×10^{-7}	0.492	0.5829
Chen (1979)	2.03×10^{-9}	0.097	0.6531
Eck (1973)	4.64×10^{-7}	1.503	0.559
Barr (1981)	1.95×10^{-9}	0.063	0.6616
Zigrang & Sylvester (1982) Eq. (12)	7.07×10^{-11}	0.019	0.6735
Churchill (1977)	2.19×10^{-7}	0.475	0.604
Wood (1966)	5.91×10^{-6}	3.876	0.525
Manadilli (1997)	1.28×10^{-7}	0.393	0.6514
Round (1980)	1.84×10^{-5}	4.474	0.5795
Buzzelli (2008)	5.62×10^{-12}	0.005	0.6922
Avci & Karagoz (2009)	3.35×10^{-6}	1.716	0.6122
Moody (1947)	7.14×10^{-5}	6.098	0.4892
Romeo *et al.* (2002)	1.33×10^{-9}	0.057	0.711
Tsal (1989)	1.75×10^{-4}	8.894	0.5675
Brkić (2011) Eq. (B)	1.35×10^{-7}	0.479	0.6735
Altshul cited in Genić *et al.* (2011)	1.75×10^{-4}	11.449	0.4773
Papaevangelou *et al.* (2010)	4.09×10^{-8}	0.23	0.7399
Brkić (2011), Eq. (A)	1.51×10^{-7}	0.721	0.6939
Rao & Kumar (2007)	5.16×10^{-5}	13.27	0.6854

efficient and slower compared to Swamee–Jain. On the other hand, Gregory & McEnery (2017) developed and tested against data generated from the accepted standard for predicting the coefficient of friction in Moody's diagram, an equation for accurately predicting the coefficient of friction without iteration. Rather, they rely on the Haaland expression, as it is more precise than the Swamee–Jain equation.

Thus from the results obtained in this work, the Swamee–Jain equation gives numerical results closer to the results calculated from the Colebrook–White expression. On the side walls of all the sections, we find the maximum friction in a range of the same thickness (4–6 mm); which results in the fact that the friction on this wall does not evolve and does not take into account the position of the geometry. Using Haaland's formula, we observe its sensitivity to the thickness of the boundary layer as a function of the velocity and the wall chosen, which is not the case for the Swamee–Jain formula. Haalands formula turns out to be more interesting for the description of the phenomenon of turbulent friction along the walls. However, the Swamee–Jain formula comes closest to the Colebrook–White equation. It should be noted that this work is carried out with clear water, and without sediment transport.

CONCLUSIONS

In this work, the focus was on determining the coefficient of friction using two approaches and finding which one best characterizes the friction and/or which gives results close to the implicit formula of Colebrook–White. Using a numerical approach

based on the CFD method, we first started with the expression developed by Haaland, and second, with the formula developed by Swamee–Jain. It appears that the Haaland equation better describes the evolution of friction because it has a more sensitive character than that of Swamee–Jain on phenomena near the walls. However, the Swamee–Jain equation gives numerical results closer to the results calculated from the Colebrook–White expression. Regarding the thicknesses at which the friction is maximum, the Swamee–Jain correlation gives substantially identical results for different velocities on the lower and upper walls. On the other hand, these thicknesses vary as a function of the velocity in the Haaland correlation. Regarding the side wall, the two formulas give the same height for the coefficient of friction. Likewise, we note that the average height for a value of the maximum coefficient of friction varies according to the geographical disposition of the penstock portion.

ACKNOWLEDGEMENTS

We sincerely acknowledge IUG-Cameroon that eased the realization of this work, and pay homage to its founder Louis-Marie DJAMBOU (rest in peace) who opened the door to his institution.

FUNDING

The authors declare that no funds, grants, or other support were received during the preparation of this manuscript.

AUTHOR CONTRIBUTIONS

All authors have read and approved the final manuscript.

ETHICAL STATEMENT

Free and informed consent of the participants or their legal representatives was obtained.

DATA AVAILABILITY STATEMENT

All relevant data are included in the paper or its Supplementary Information.

CONFLICT OF INTEREST

The authors declare there is no conflict.

REFERENCES

Achour, B. & Bedjaoui, A. (2006) Calcul du coefficient de frottement en conduite circulaire sous pression, *Larhyss Edition Capitale, ISSN 1112-3680*, **5**, 197–200.

Avci, A. & Karagoz, I. (2009) Discussion: A novel explicit equation for friction factor in smooth and rough pipes, *ASME Journal of Fluids Engineering*, **131**, 061203.

Barr, D. I. H. (1981) Solutions of the Colebrook-White functions for resistance to uniform turbulent flows, *Proceedings of the Institution of Civil Engineering*, **71**, 529–536.

Brkic, D. (2011) An explicit approximation of the Colebrook equation for fluid flow friction factor, *Petroleum Science and Technology*, **29**, 1596–1602.

Buzzelli, D. (2008) Calculating friction in one step, *Machine Design*, **80**, 54–55.

Boussinesq, J. (1877) *Théorie de L'écoulement Tourbillonnant et Tulmultueux des Liquides dans les Lits Rectilignes à Grande Section*, 2 vols. Fautiers-Villars, Paris.

Chapallaz, J. M., Mombell, H. P., Renaud, A., Scheder, J. C. & Graf, J. (1995) *Le choix, dimensionnement et les essais de reception d'une mini-turbine*. Programme d'action PACER – Energies renouvelables, Office fédéral des questions conjoncturelles, ISBN 3-905232-57-8, N0724.247.4f, 73 pages.

Chen, N. H. (1979) An explicit equation for friction factors in pipes, *Industrial & Engineering Chemistry Fundamentals*, **18**, 296–297. http://dx.doi.org/10.1021/i160071a019

Churchill, S. W. (1973) Empirical expressions for the shear stress in turbulent flow in commercial pipe, *AIChE J* **19**, 375-376.

Churchill, S. W. (1977) Friction factor equation spans all fluid-flow ranges, *Chemical Engineering*, **84**, 91–92.

Colebrook, C. F. (1939) Turbulent flow in pipes with particular reference to the transition region between the smooth and rough pipe laws, *Journal of the Institution of Civil Engineers*, **11**, 133–156.

Colebrook, C. F. & White, C. M. (1937) Experiments with fluid friction in roughened pipes, *Proceedings of the Royal Society of London. Series A*, **161**, 367.

Elie, F. (2014) *Les Conduites Forcées: Principes, Aménagements, Sécurités*. researchgate.net/publication/3161, Frédéric Elie on ResearchGate ©Frédéric Élie – http://fred.elie.free.fr, mai 2014, Marseille.

Eck, B. (1973) *Technische Stromungslehre.* Springer, New York.

Fang, Y. H., Chiu, C. M. & Wang, E. T. G. (2011) Understanding customers' satisfaction and repurchase intentions: An integration of IS success model, trust, and justice, *Internet Research*, **21**, 479–503. http://dx.doi.org/10.1108/10662241111158335

Genić, S., Arandjelović, I., Kolendić, P., Jsrić, M. & Budimir, N. (2011) A review of explicit approximations of Colebrook's equation, *FME Tranactions,* **39**, 67–71.

Gregory, J. M. & McEnery, J. A. (2017) Process-Based friction factor for pipe flow open, *Journal of Fluid Dynamics*, **7**, 219–230. doi:10.4236/ojfd.2017.72015.

Haaland, S. (1983) Simple and explicit formulas for the friction factor in turbulent pipe flow, *Journal Fluids Engineering*, **105**, 89–90. doi:10.1115/1.3240948.

Jain, A. K. (1976) Accurate explicit equation for friction factor, *Journal for the Hydraulic Division American Society of Civil Engineers*, **102**, 674–677.

Ketcheuzeu-Ngakam, J., Koueni-Toko, C., Djeumako, B., Tcheukam-Toko, D. & Kuitche, A. (2014) Characterization of hydrodynamics parameters of a Kaplan turbine, *Energy and Power*, **4** (3), 58–69. DOI: 10.12691/ajer-6-2-1.

Manadilli, G. (1997) Replace implicit equations with signomial functions, *Chemical Engineering*, **104**, 129–132.

Moody, L. F. (1947) An approximate formula for pipe friction factors, *Transactions of the American Society of Mechanical Engineers*, **69**, 1005–1006.

Papaevangelou, G., Evangelides, C. & Tzimopoulos, C. (2010) A new explicit relation for friction coefficient in the Darcy-Weisbach equation, *Proceedings of the Tenth Conference on Protection and Restoration of the Environment*, **166**, 1–7. PRE10 July 6-09 2010 Corfu, Greece.

Prandtl, L. (1932) Zur turbulenten Strömung in Rohren und längs Platten, In: *Ergebnisse der Aerodynamischen Versuchsanstalt zu Göttingen*, **4**, 18–29. LPGA 2, 632–648. available at http:/www.cambridge.org/core/terms. http://dx.doi.org/10.1017/CBO9781139018241.003

Rao, A. R. & Kumar, B. (2007) *Friction Factor for Turbulent Pipe Flow*. Division of Mechanical Sciences, Civil Engineering Indian Institute of Science, Bangalore, ID Code 9587.

Romeo, E., Royo, C. & Monzón, A. (2002) Improved explicit equations for estimation of the friction factor in rough and smooth pipes, *Chemical Engineering Journal*, **86**, 369–374.

Round, G. F. (1980) An explicit approximation for the friction factor-Reynolds number relation for rough and smooth pipes, *Canadian Journal of Chemical Engineering*, **58**, 122–123.

Schorle, B. J., Churchill, S. W. & Shacham, M. (1980) Comments on: An explicit equation for friction factor in pipe, *Industrial & Engineering Chemistry Fundamentals*, **19**, 228–229. http://dx.doi.org/10.1021/i160074a019

Seghides, T. K. (1984) Estimate friction factor accurately, *Chemical Engineering Journal*, **91**, 63–64.

Sonnad, J. R. & Goudar, C. T. (2006) Turbulent flow friction factor calculation using mathematically exact alternative to the Colebrook-White equation, *Journal of the Hydraulic Division American Society of Civil Engineers*, **132**, 863–867.

Swamee, P. K. & Jain, A. K. (1976) Explicit equations for pipe-flow problems, *Journal of the Hydraulics Division*, **102** (5), 657–664.

Tchawe, T. M., Djeumako, B., Koueni-Toko, C., Tcheukam-Toko, D. & Kuitche, A. (2015) Study of dynamic field around a vertical circular cylinder placed in an open-Chanel flow, *International Journal of Innovative Science, Engineering & Technology*, **2**, 6.

Tchawe, T. M., Djiako, T., Kenmeugne, B. & Tcheukam-Toko, D. (2018) Numerical study of the flow upstream of a water intake hydroelectric Dam in stationary regime, *American Journal of Energy Research*, **6** (2), 35–41. doi:10.12691/ajer-6-2-1.

Tsal, R. J. (1989) Altshul-Tsal friction factor equation, *Heating Piping Air Conditioning* **8**, 30-45.

Von Karman, T. (1934) The fundamentals of the statistical theory of turbulence, *Journal of Aeronautical Science*, **4**, 131–138.

Wang, C., Meng, T., Hu, H. & Zhang, L. (2012) Accuracy of the ultrasonic flow meter used in the hydroturbine intake penstock of the three gorges power station, *Flow Measurement and Instrumentation*, **25**, 32–39. doi:10.1016/j.flowmeasinst.2011.12.003.

Wilcox, D. (1998) *Turbulence Modeling for CFD*, 2nd edn. DCW Industries, Inc, La Canada, California.

Winning, H. & Coole, T. (2015) Improved method of determining friction facteur in pipes, *International Journal of Numerical Method for Heat & Fluid Flow*, **25** (5), 914–999.

Wood, D. J. (1966) *An Explicit Friction Factor Relationship*. Civil Engineering, American Society of Civil Engineers, Reston, VA, pp. 60–61.

Zigrang, D. J. & Sylvester, N. D. (1982) Explicit approximations to the solution of Colebrook's friction factor equation, *AIChE Journal*, **28**, 514–515. http://dx.doi.org/10.1002/aic.690280323

First received 11 April 2024; accepted in revised form 29 August 2024. Available online 18 September 2024